ACS APPLIED MATERIALS & INTERFACES

Research Article

www.acsami.org

Fluorescence Resonance Energy Transfer in a Binary Organic Nanoparticle System and Its Application

Meng Wu, Xinjun Xu,* Jinshan Wang, and Lidong Li*

School of Materials Science and Engineering, University of Science and Technology Beijing, Beijing 100083, P. R. China

Supporting Information

ABSTRACT: Fluorescent organic nanoparticles have a much better photostability than molecule-based probes. Here, we report a simple strategy to detect chemicals and biomolecules by a binary nanoparticle system based on fluorescence resonance energy transfer (FRET). Poly(9,9-di-*n*-octylfluorenyl-2,7-diyl) (PFO, energy donor) and poly [2-methoxy-5-(2-ethylhexyloxy)-1,4-phenylenevinylene] (MEH-PPV, energy acceptor) are utilized to prepare the binary nanoparticle system through a reprecipitation method. Since the FRET process is strongly distance-dependent, a change in the interparticle distance between the two kinds of nanoparticles after introduction of analytes will alter the FRET efficiency. The response of the binary nanoparticle system to cationic polyelectrolytes was investigated by monitoring the FRET efficiency from PFO to MEH-PPV nanoparticles and the fluorescence color of the nanoparticle solutions. Furthermore, the cationic polyelectrolyte pretreated binary nanoparticle system can be used to detect DNA by desorption of nanoparticles from the polyelectrolyte's chains and the detection concentration can go down to 10^{-14} M. Thus, the binary nanoparticle system shows great promise for applications in chemical sensing or biosensing.

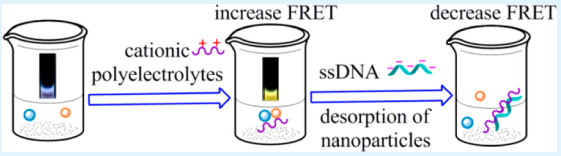

KEYWORDS: *fluorescence, conjugated polymer, fluorescence resonance energy transfer, polyelectrolyte, organic nanoparticles, reprecipitation*

INTRODUCTION

Intramolecular and intermolecular fluorescence resonance energy transfer (FRET) is one of the most widely used sensing mechanisms for ratiometric fluorescent (FL) probes.[1−4] FRET is a nonradiative process in which an excited dye donor transfers energy to a dye acceptor in the ground state through long-range dipole−dipole interactions. When used in fluorescence sensing, it has the characteristic of distance-dependent emission, two-color fluorescence correlation, and good sensitivity.[5] Nowadays, numerous FRET-based fluorescent probes including conjugated polymers nanoparticles, small molecules, water-soluble conjugated polymer, quantum dots, and upconversion nanoparticles (NPs) have been exploited to detect either biomolecules such as proteins and nucleic acids or chemicals such as toxins, active oxygen species, and metal ions.[6−13] Most of these fluorescent probes are small molecules or water-soluble conjugated polymers.[1,14−16] However, such molecular probes often suffer from low photostability such as photoblinking, photobleaching, and photooxidation.[17,18]

In recent years, fluorescent organic nanoparticles (FONs) have attracted much attention since they own unique optical properties.[19−21] Compared with molecular systems such as conjugated polymers, FONs have advantages of good photostability and easy surface functionalization, which are important in the applications of fluorescence detection. In comparison with metal NPs, inorganic quantum dots (QDs), and upconversion NPs, organic nanoparticles are easy to prepare by methods such as reprecipitation and miniemulsion,[19] and the raw materials are cheaper, less cytotoxic, and easier to be modified.[19,20,22−31] Many kinds of fluorescent organic materials can be chosen to fabricate FONs including small molecules,[32] oligomers,[33] and fluorescent polymers.[34,35] By contrast, most of the reported QD approaches required covalent conjugation of DNA to the quantum dots, which often decreases the colloidal stability and the emission intensity of QDs.[12] Currently, FONs are utilized in aqueous solutions as chemical sensors,[36] photosensitizers,[37,38] biosensors,[39,40] and cell imaging agents.[41,42] Nevertheless, almost all the reported FON probes are based on a unitary nanoparticle system where FRET can hardly be utilized to play a role in sensing. Due to the validity and sensitivity of FRET in fluorescent sensing, which have already be widely verified in molecule-based systems, it is expected that a binary nanoparticle system can be exploited for chemo-/biosensing, where both the merits of FRET and photostability can be combined.

Nowadays, the existing methods for DNA detection include polymerase chain reaction (PCR), immunoassays, and fluorescent dye molecules. Although these approaches are convenient, their detection limits are not good.[43,44] The FRET based probes currently used for ssDNA mainly contain QDs, upconversion NPs, and water-soluble conjugated polymers. The detection limits are usually in the range of 10^{-9}−10^{-8} M.[12,13,45] The other mainstream detection technique is gold nanoparticle based detection and the detection limit can reach 10^{-12} M.[17,46]

Received: February 10, 2015
Accepted: March 31, 2015
Published: March 31, 2015

DOI: 10.1021/acsami.5b01338
ACS Appl. Mater. Interfaces 2015, 7, 8243−8250

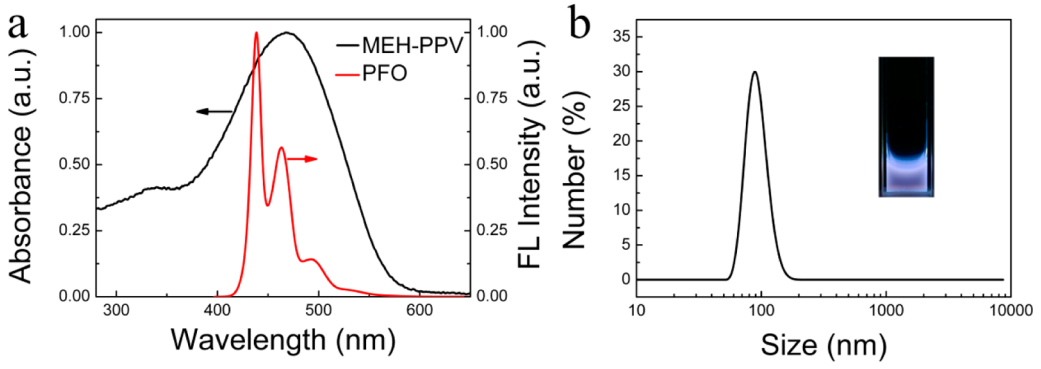

Figure 1. (a) FL emission spectra of PFO nanoparticles and UV−vis absorption spectra of MEH-PPV nanoparticles. (b) Size (diameter) distribution of the binary nanoparticle system (PFO+MEH-PPV dispersed in aqueous solution). The inset shows the photograph of this solution under UV (365 nm) irradiation.

In this paper, we utilize a binary nanoparticle system composed of conjugated polymers to respond cationic polyelectrolytes and trace amount of single-strand DNAs (ssDNAs) via FRET mechanism. Poly(9,9-di-*n*-octylfluorenyl-2,7-diyl) (PFO) and poly[2-methoxy-5-(2-ethylhexyloxy)-1,4-phenylenevinylene] (MEH-PPV) are employed to serve as the building materials for FONs. The reprecipitation method is utilized to fabricate the binary nanoparticle system with blended PFO and MEH-PPV nanoparticles in aqueous solution. FRET will occur between the two kinds of nanoparticles within an appropriate distance. We found that, in aqueous solution, PFO and MEH-PPV nanoparticles have negative surface charges and cationic polyelectrolytes can shorten the distance among neighboring nanoparticles, which can increase the FRET efficiency between the two kinds of nanoparticles. Therefore, we can use this binary nanoparticle system to respond cationic polyelectrolytes. Furthermore, since ssDNA has high density of negative charges, an electrostatic interaction may be expected to occur with the polymeric chain of polyelectrolytes. Consequently, ssDNAs can desorb the nanoparticles from the chains of polyelectrolytes and the FRET efficiency between the two kinds of nanoparticles will decrease. As a result, by using this strategy, we can realize an ultrasensitive detection of ssDNAs with a limiting concentration down to 10^{-14} M.

EXPERIMENTAL METHODS

Materials. Poly(9,9-di-*n*-octylfluorenyl-2,7-diyl) (PFO) (M_n = 15 834, M_w = 58 200), poly[2-methoxy-5-(2-ethylhexyloxy)-1,4-phenylenevinylene] (MEH-PPV) (M_n = 40 000−70 000), poly(ethylenimine) (PEI) (M_w = 750 000), poly(diallydimethylammonium chloride) (PDDA) (M_w = 200 000 to 350 000), poly(acrylic acid) (PAA) (M_w = 100 000), poly(allylamine hydrochloride) (PAH) (M_w = ~58 000), and poly(styrenesulfonate) sodium (PSS) (M_w = 70 000) were obtained from Sigma-Aldrich Co. Poly(L-lysine)hydrobromide (PLL) (M_r = 70 000 to 150 000) was purchased from Bio Dee Biotechnology Co., Ltd. All of the chemicals were used as received without any further purification. The oligonucleotides were purchased from Sangon Biotech (Shanghai) Co., Ltd. Tetrahydrofuran (THF) and ultrapure deionized water (18.3 MΩ) were used as the solvents in the experiments. Fluorescent emission and ultraviolet−visible (UV−vis) absorption spectra were obtained using a Hitachi F-7000 fluorescence spectrometer and a Hitachi U-3900H spectrophotometer, respectively, at room temperature. The zeta-potential and average hydrodynamic diameters of the nanoparticles were measured using a Nano ZS90 instrument (Malvern Instrument Ltd.) in solutions at room temperature. Fluorescence images of nanoparticles were recorded using an Olympus FV1000-IX81 confocal laser scanning microscope with an excitation wavelength of 385 nm and a capture range above 420 nm. The optical photographs of nanoparticle suspensions in cuvettes were taken under the irradiation of 365 nm light produced by an ultraviolet (UV) lamp.

Preparation of the Binary Nanoparticle System and Optical Characterization. PFO and MEH-PPV blended NPs were fabricated through a reprecipitation method.[23] Briefly, the conjugated polymers were dissolved in THF in the dark to form molecule-dispersed solutions with a concentration of 2.0 mg/mL. Thereafter, they were filtered by 0.22 μm polyvinylidene fluoride (PVDF) filters. After that, 250 μL of the PFO THF solution was rapidly injected into 5 mL of deionized water (18.3 MΩ) at 45 °C under ultrasonication for 5 min. Then, 250 μL of the MEH-PPV THF solution was rapidly injected into the former nanoparticle solution at 45 °C under ultrasonication for another 5 min. This solution was then filtered through a 0.22 μm poly(tetrafluoroethylene) (PTFE) filter.

Polyelectrolyte Response Assay of the Nanoparticles. The binary nanoparticle solution was incubated for 12 h in order to be well-mixed. After that, 500 μL of the binary nanoparticle solution was injected into six quartz cuvettes, respectively. Then, 200 μL of deionized water was added to each cuvette to dilute the above nanoparticle solution. Various polyelectrolytes have been investigated including PLL, PAH, PDDA, PEI, PSS, and PAA. They were injected into the six diluted solutions with the final concentration ranged from 1×10^{-6} to 1×10^{-4} M (calculated on repeating unit concentration). The fluorescent emission spectra were obtained with an excitation wavelength of 385 nm.

ssDNA Detection. 500 μL of the binary nanoparticle solution was put into two quartz cuvettes. Then, 200 μL of deionized water was added to both cuvettes to dilute the above solutions. After that, PLL was injected into one of the nanoparticle solutions with a final concentration of 1×10^{-5} M. Then, ssDNA was injected into the nanoparticle solutions (both with and without PLL pretreatment) to get a final DNA concentration from 1×10^{-14} to 5×10^{-12} M. Fluorescent spectra were measured with an excitation wavelength of 385 nm.

Fluorescence Images. First, coverslips were cleaned up by distilled water and then treated by piranha solution (H_2O_2:H_2SO_4 = 1:2 v/v) for 1 h. Then, the coverslips were washed with ultrapure deionized water for three times and dried under a gentle stream of nitrogen gas. The fluorescence images were then obtained by dropping 2 μL of the corresponding solutions, which are the binary nanoparticle solutions without any additives, with PLL, and with PLL+ssDNA, onto the cleaned coverslips.

RESULTS AND DISCUSSION

Characterization of Nanoparticles in Aqueous Solution. FRET is the physical process by which energy is transferred nonradiatively from an excited molecular chromophore (the donor, D) to another chromophore (the acceptor,

DOI: 10.1021/acsami.5b01338
ACS Appl. Mater. Interfaces 2015, 7, 8243−8250

A) by means of intermolecular long-range dipole−dipole coupling. The essential requirements for effective transfer are that the distance is from 1 to 10 nm and that the fluorescence spectrum of the donor and the absorbance spectrum of the acceptor overlap adequately.[47] In general, PFO exhibits a blue emission and shows a dominant peak at 425 nm with shoulders at 457 and 489 nm.[48] Pristine MEH-PPV exhibits orange color with the dominant peak above 550 nm and a shoulder peak at 598 nm in a hydrous THF solution.[49] As shown in Figure 1a, MEH-PPV nanoparticles demonstrate a broad UV−vis absorption band in the range of 300−580 nm which overlaps well with the emission band of PFO nanoparticles. According to the calculation, the Forster radius R_0 is ∼6 nm (see details in Supporting Information). As a result, an FRET process may be expected to occur in the binary nanoparticle system given that the interparticle distance is appropriate. Figure 1b shows the size distribution of the blended PFO and MEH-PPV nanoparticles in aqueous solution. These nanoparticles have a mean particle size of 94.3 nm (with a polydispersity index of 0.114). The nanoparticle solution is very stable even over 1 month with no evidence of aggregation. These nanoparticles can be stabilized in aqueous solution by the repulsive electrostatic force between particles due to the same kind of surface charges they carried. According to Coehn's empirical rule, when two dielectrics are in intimate contact, the electrostatic charge separation may occur. The substance with higher dielectric constant will receive the positive charge, while the other one will receive the negative charge.[50,51] The relative dielectric constant of water is 80, while that of PFO and MEH-PPV is 3.26 and 3.0, respectively.[52,53] As a result, negative charges should form on the surface of PFO and MEH-PPV nanoparticles in aqueous solution. As verified from the ζ potential measurement, the value of the binary nanoparticle suspension is−25.2 mV.

Response of the Binary Nanoparticle System to Polyelectrolytes. As mentioned above, nanoparticles in the aqueous solution have negative surface charges. Therefore, they can be absorbed onto the polymeric chains of cationic polyelectrolytes and thus be expected to demonstrate a fluorescence change. To verify this hypothesis, either cationic polyelectrolytes including PLL, PAH, PEI, and PDDA or anionic polyelectrolytes including PSS and PAA were investigated under identical conditions. Figure 2 shows the molecular structures of these polyelectrolytes. Figure 3 shows the FL emission spectra for the binary nanoparticle aqueous solutions with different concentrations of polyelectrolytes and the insets show the photographs of the nanoparticle aqueous solutions either untreated or treated by the polyelectrolytes. They were all normalized at the wavelength of 437 nm. The emission bands in the short wavelength (blue light) region came from the PFO emission and those in the long wavelength (orange light) region arose from the MEH-PPV emission.

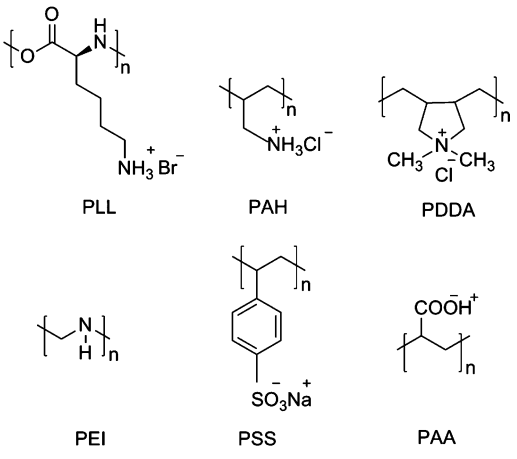

Figure 2. Molecular structures of the polyelectrolytes.

With increasing the concentration of cationic polyelectrolytes (PLL, PAH, PEI, and PDDA) in the binary nanoparticle system, the emission intensity of MEH-PPV becomes larger and larger relative to that of PFO (Figure 3a−d). In addition, the emission colors of the solutions are obviously changed from blue to yellow (shown in the insets of Figure 3a−d). However, for the anionic polyelectrolytes (PSS and PAA), it is a different case. With increasing the concentration of anionic polyelectrolytes in the binary nanoparticle system, the emission intensity of MEH-PPV is only slightly changed relative to that of PFO and the emission colors of the solutions are almost unchanged (Figure 3e and f). As mentioned above, both PFO and MEH-PPV nanoparticles have negative surface charges, while cationic polyelectrolytes have positive charges in the polymeric chains. Introduction of cationic polyelectrolytes into the binary nanoparticle system will move the nanoparticles close to each other, mediated through the electrostatic adsorption between nanoparticles and polymeric chains. Because FRET is distance dependent, a reduced distance among nanoparticles in the aqueous solution will enhance the FRET efficiency from PFO to MEH-PPV, leading to an increase in the emission intensity of MEH-PPV nanoparticles. As for anionic polyelectrolytes, since they carry negative charges the same as PFO and MEH-PPV nanoparticles, there is no electrostatic adsorption occurring and the distance between the two kinds of nanoparticles can hardly be reduced. Therefore, the FRET efficiency has no obvious change. As shown in Figure 4, the FRET ratio (defined here as the fluorescent intensity ratio of $I_{574\ nm}/I_{437\ nm}$) in the binary nanoparticle system without any additives is 0.23, while the FRET ratios of the binary nanoparticle system with the addition of PLL, PDDA, PAH, PEI, PSS, and PAA (with the final concentration of 1×10^{-4} M) are 1.59, 1.15, 1.01, 0.99, 0.25, and 0.22, respectively. As reflected by the ratios of $I_{574\ nm}/I_{437\ nm}$, the FRET efficiency in the binary nanoparticle system with the addition of cationic polyelectrolytes increases at least 3.3 times over that before addition of polyelectrolytes, and a maximum increase of 6 times is achieved when treated by PLL.

As seen from Figure 2, the repetitive unit of PLL has two amino groups. Both of them can be hydrolyzed in aqueous solutions to carry positive charges, while each repetitive unit of PAH, PDDA, and PEI only has one amino group to be hydrolyzed. So PLL has a higher charge density than the other cationic polyelectrolytes in the same repetitive unit concentration. Thus, the electrostatic interaction between PLL and nanoparticles is stronger than other cationic polyelectrolytes, leading to the intensity of MEH-PPV being a little higher when PLL is added.

However, the FRET efficiency in the binary nanoparticle system treated by anionic polyelectrolytes has little change. As a result, it demonstrates that the PFO and MEH-PPV binary nanoparticle system has a response to cationic polyelectrolytes.

DNA Detection in Aqueous Solution. Since the binary nanoparticle system with the addition of PLL can exhibit the best enhancement in FRET efficiency, we selected PLL for the

DOI: 10.1021/acsami.5b01338
ACS Appl. Mater. Interfaces 2015, 7, 8243−8250

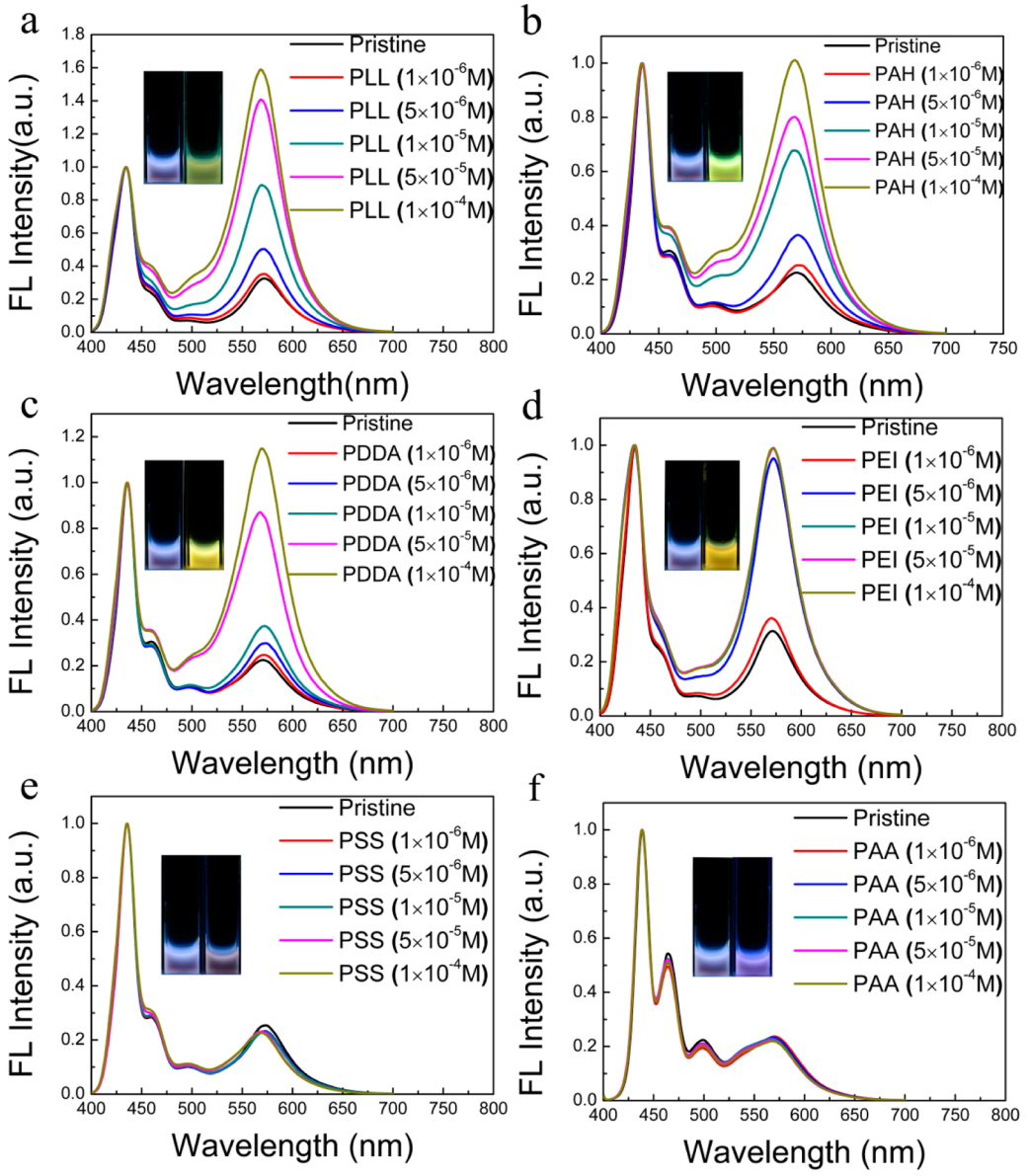

Figure 3. FL emission spectra of the binary nanoparticle system with different concentrations of polyelectrolytes: (a) PLL, (b) PAH, (c) PDDA, (d) PEI, (e) PSS, and (f) PAA. The insets show the photographs of UV-radiated nanoparticle aqueous solutions either untreated (pristine) (left) or treated by the polyelectrolyte (1×10^{-4} M) (right). Spectra were normalized at 437 nm and the excitation wavelength was fixed at 385 nm.

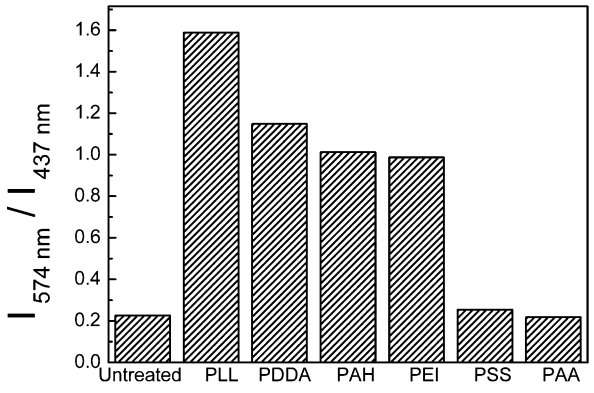

Figure 4. FRET ratio $I_{574\ nm}/I_{437\ nm}$ for the binary nanoparticle system in aqueous solutions which are either untreated or treated by PLL, PDDA, PAH, PEI, PSS, and PAA with the final concentration of 1×10^{-4} M, respectively.

following experiment. In this experiment, the binary nanoparticle system pretreated by PLL was used to detect DNA. As an example, the ssDNA of A43 (CTGACATACTAGCACGTCCTATATCTTCTCGTCTCGTAGACGT) was injected into the binary nanoparticle solutions which were either untreated or treated with PLL. Since ssDNA carries negative charges, when injected into the pristine binary nanoparticle system, the FRET efficiency should have almost no change, similar to the case of anionic polyelectrolytes. This can be verified from Figure 5a, where only a very small degree of quenching is observed in the FL emission of MEH-PPV. In addition, the FRET efficiency changes only slightly as the concentration of ssDNA was varied from 1×10^{-14} to 5×10^{-12} M. However, when ssDNA is injected into the binary nanoparticle system pretreated by PLL (1×10^{-5} M), the FRET efficiency is decreased. As shown in Figure 5b, with increasing concentrations of ssDNA, the FRET ratio ($I_{574\ nm}/I_{437\ nm}$) in the binary nanoparticle system with PLL pretreat-

DOI: 10.1021/acsami.5b01338
ACS Appl. Mater. Interfaces 2015, 7, 8243−8250

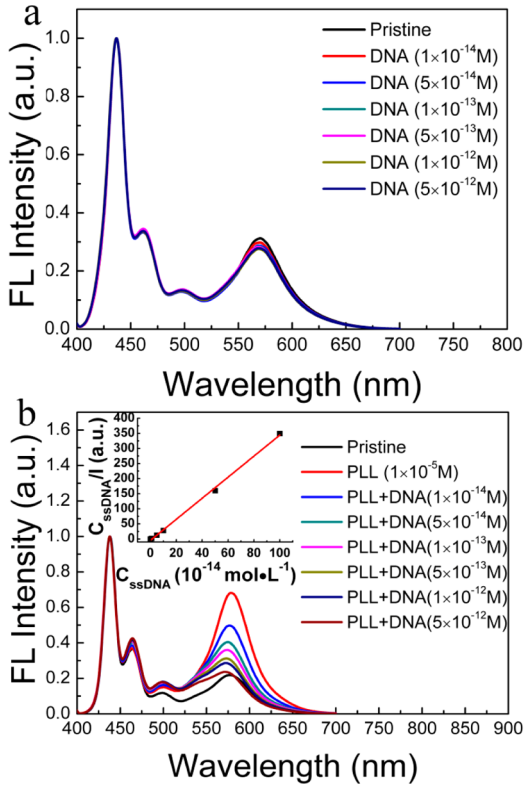

Figure 5. FL emission spectra for the binary nanoparticle system, which was either untreated by PLL (a) or pretreated by PLL (1×10^{-5} M) (b), with different concentrations of ssDNA. The inset in (b) shows the relationship of MEH-PPV's intensity (I) to the concentration of ssDNA (C_{ssDNA}), which is in accord with the Langmuir adsorption isotherm. FL spectra were normalized at 437 nm and the excitation wavelength was fixed at 385 nm.

ment gradually decreases and is reduced from the initial value of 0.680 to 0.236 when the ssDNA concentration reaches 5×10^{-12} M, which is nearly equal to that of the pristine binary nanoparticle system without any additives. It should be noted that, even when the ssDNA concentration is extremely low (1×10^{-14} M) in the binary nanoparticle system pretreated by PLL, an obvious decrease in the fluorescent intensity of MEH-PPV relative to that of PFO can still be observed (27% reduction). Compared with the other methods, such as QDs, upconversion NPs, gold NPs with the detection limits in the range of 10^{-9}–10^{-12} M, our method shows a much better detection limit.[12,13,46]

Since ssDNA has a high negative charge density, it can bind more strongly to the chains of cationic polyelectrolytes than PFO and MEH-PPV nanoparticles. As a result, nanoparticles can be desorbed from the polymeric chains of PLL after injecting A43 into the binary nanoparticle solution and the distance between PFO and MEH-PPV nanoparticles became larger than before. Consequently, the FRET efficiency decreased. As confirmed by the ζ potential measurement, the binary nanoparticle system exhibited a value of 23.1 mV with PLL pretreatment, while it decreased to 1.7 mV when ssDNA was introduced (5×10^{-12} M). By drawing a curve with C_{ssDNA}/I versus C_{ssDNA}, where C_{ssDNA} is the concentration of ssDNA and I is the FL intensity of MEH-PPV in Figure 5b, we found that a linear relationship existed (see the inset of Figure 5b). This result resembles the Langmuir adsorption isotherm,[54,55] indicating that the binding of ssDNA to PLL coincides with the Langmuir adsorption model.

When injecting ssDNA with different sequence lengths into the binary nanoparticle system pretreated by PLL (1×10^{-5} M), the FRET efficiency are different. The system responses better to ssDNA with larger lengths. As seen from Figure 5b and Figure S1, with increasing concentrations of ssDNA, the FRET ratio ($I_{574\ nm}/I_{437\ nm}$) of A43 decreased obviously, the FRET ratio ($I_{574\ nm}/I_{437\ nm}$) of P25 (ATCGCTAGAAAACCC-TTTATCGCTA) only had a slight decrease, and the FRET ratio ($I_{574\ nm}/I_{437\ nm}$) of P7 (AAAACCC) had almost no change. So this method can distinguish DNA sequences with different lengths.

Confocal Laser Scanning Microscope Images of the Binary Nanoparticle System. The real-color fluorescence images (Figure 6a and b) of the binary nanoparticle system without and with the addition of PLL were measured by confocal laser scanning microscope (CLSM). As shown in Figure 6a, in the absence of PLL, the aggregation degree of nanoparticles is small and the fluorescence brightness of MEH-PPV is faint. Because both kinds of FONs are of good dispersibility in solution (shown in Figure 1b), it should be noted that the aggregation of nanoparticles described here is not an irreversible process and should be considered a temporary event occurring during the imaging period. After injection of PLL into the binary nanoparticle solution, the cationic polyelectrolyte can shorten the distance between PFO and MEH-PPV nanoparticles. As a result, the FRET efficiency can increase, which can be verified from Figure 6b. In this image, more particles with brighter orange fluorescence can be observed and the aggregation degree of nanoparticles becomes large. Due to the electrostatic interactions between PLL (with positive charges in its chain) and nanoparticles (with negative charges on their surfaces), the distance among nanoparticles can be shortened with the help of polymeric chains and some nanoparticles can even be wrapped by PLL. Consequently, a large degree of nanoparticle aggregation can be observed. In such aggregations, PFO and MEH-PPV NPs approach very close to each other and a short distance of less than 10 nm may be guaranteed, so FRET can occur efficiently. Figure 6c shows the fluorescence image of the PLL pretreated binary nanoparticle system with the addition of ssDNA. When ssDNA (A43) was injected into the PLL pretreated binary nanoparticle system, the oligonucleotides which carry a high negative charge density can bind to the polymeric chains of PLL and allow PFO and MEH-PPV nanoparticles to be desorbed. As can be seen from Figure 6c, the aggregation degree of the nanoparticles became small again, which means the distance among nanoparticles becomes large and the fluorescence brightness of the MEH-PPV nanoparticles turns weak. In addition, as seen from Figure 6d, the dominated hydrodynamic diameter is 94.3 nm for the binary nanoparticle system in the absence of PLL and it changes to 141.8 nm with the presence of PLL. After injection of the ssDNA (A43) into the PLL pretreated binary nanoparticle system, the hydrodynamic diameter recovered to a similar value as that in the pristine one. As a result, the binary nanoparticle system pretreated by cationic polyelectrolyte has a good response to the trace amount of ssDNA.

CONCLUSION

Conjugated polymer nanoparticles with good dispersibility were produced using the reprecipitation method. They have been explored for cationic polyelectrolyte response and trace

DOI: 10.1021/acsami.5b01338
ACS Appl. Mater. Interfaces 2015, 7, 8243–8250

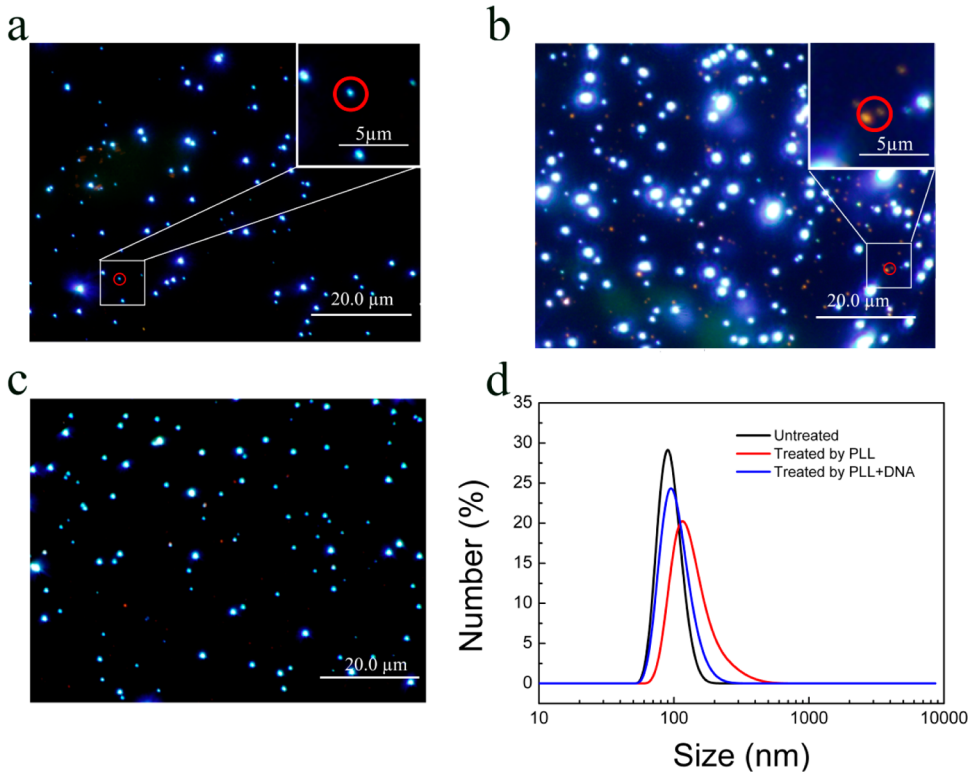

Figure 6. CLSM micrographs of the binary nanoparticle system (PFO and MEH-PPV nanoparticles) without additives (a), with addition of PLL (1×10^{-5} M) (b), and with addition of PLL (1×10^{-5} M) + ssDNA (5×10^{-12} M) (c). (d) Size (diameter) distribution of nanoparticles in aqueous solutions corresponding to those shown in (a)−(c). The insets in (a) and (b) are the partial enlargement for the rectangle region.

amount of DNA detection. A binary nanoparticle system comprising PFO and MEH-PPV nanoparticles responded well to cationic polyelectrolytes such as PLL, PAH, PEI, and PDDA by monitoring the FRET efficiency from PFO to MEH-PPV nanoparticles; however, it was inert to anionic polyelectrolytes. The higher the cationic polyelectrolyte concentration is, the more efficient the FRET process becomes. The FRET efficiency in the binary nanoparticle system is reflected by the fluorescent intensity ratio ($I_{574\ nm}/I_{437}$). An enhancement in the FRET efficiency of at least 3.3-fold has been observed with the addition of cationic polyelectrolytes (1×10^{-4} M), especially with the addition of PLL which exhibited a maximum increase of 6-fold. Furthermore, this response can be utilized to detect ssDNA. The ability of detecting ssDNA by the PLL pretreated binary nanoparticle was also investigated by monitoring the FRET efficiency from PFO to MEH-PPV nanoparticles. With the injection of ssDNA (A43), the FRET ratio ($I_{574\ nm}/I_{437}$) had obviously decreased, which is in accord with the Langmuir adsorption isotherm. In the PLL pretreated binary nanoparticle system, the distance among nanoparticles and brightness of MEH-PPV nanoparticles before and after addition of ssDNA were different in the CLSM images. Even a trace amount of ssDNA as low as 1×10^{-14} M can be detected by using this strategy. Therefore, we believe that the binary nanoparticle system based on FRET provides a new avenue for the ultrasensitive DNA detection.

■ ASSOCIATED CONTENT

Supporting Information

The fluorescent emission spectra for the binary nanoparticles pretreated by PLL with different concentrations of ssDNA (P25) and ssDNA (P7) in aqueous solution. The calculation of the related FRET parameters. This material is available free of charge via the Internet at http://pubs.acs.org.

■ AUTHOR INFORMATION

Corresponding Authors

*E-mail: xuxj@mater.ustb.edu.cn.
*E-mail: lidong@mater.ustb.edu.cn.

Notes

The authors declare no competing financial interest.

■ ACKNOWLEDGMENTS

This work is supported by the National Natural Science Foundation of China (51273020, 51373022), and Research Fund for the Doctoral Program of Higher Education of China (20130006110007).

■ REFERENCES

(1) Yuan, L.; Lin, W.; Zheng, K.; Zhu, S. FRET-Based Small-Molecule Fluorescent Probes: Rational Design and Bioimaging Applications. *Acc. Chem. Res.* **2013**, *46*, 1462−1473.

(2) Kikuchi, K.; Takakusa, H.; Nagano, T. Recent Advances in the Design of Small Molecule-Based FRET Sensors for Cell Biology. *TrAC, Trends Anal. Chem.* **2004**, *23*, 407−415.

(3) Feng, F.; Liu, L.; Wang, S. Fluorescent Conjugated Polymer-Based FRET Technique for Detection of DNA Methylation of Cancer Cells. *Nat. Protoc.* **2010**, *5*, 1255−1264.

(4) Hussain, S. A.; Dey, D.; Chakraborty, S.; Saha, J.; Roy, A. D.; Chakraborty, S.; Debnath, P.; Bhattacharjee, D. Fluorescence Resonance Energy Transfer (FRET) Sensor. *J. Spectrosc. Dyn.* **2015**, *5*, 7−23.

(5) Yang, J.-Y.; Yang, W. Y. Site-Specific Two-Color Protein Labeling for FRET Studies Using Split Inteins. *J. Am. Chem. Soc.* **2009**, *131*, 11644−11645.

DOI: 10.1021/acsami.5b01338
ACS Appl. Mater. Interfaces 2015, 7, 8243−8250

(6) Xu, Q.; Wu, C.; Zhu, C.; Duan, X.; Liu, L.; Han, Y.; Wang, Y.; Wang, S. A Water-Soluble Conjugated Polymer for Protein Identification and Denaturation Detection. *Chem.—Asian J.* **2010**, *5*, 2524−2529.
(7) Traina, C. A.; Bakus, R. C., II; Bazan, G. C. Design and Synthesis of Monofunctionalized, Water-Soluble Conjugated Polymers for Biosensing and Imaging Applications. *J. Am. Chem. Soc.* **2011**, *133*, 12600−12607.
(8) Gaylord, B. S.; Heeger, A. J.; Bazan, G. C. DNA Detection Using Water-Soluble Conjugated Polymers and Peptide Nucleic Acid Probes. *Proc. Natl. Acad. Sci. U. S. A.* **2002**, *99*, 10954−10957.
(9) Chen, B.; Wang, P.; Jin, Q.; Tang, X. Chemoselective Reduction and Self-Immolation Based FRET Probes for Detecting Hydrogen Sulfide in Solution and in Cells. *Org. Biomol. Chem.* **2014**, *12*, 5629−5633.
(10) He, F.; Feng, F.; Wang, S.; Li, Y.; Zhu, D. Fluorescence Ratiometric Assays of Hydrogen Peroxide and Glucose in Serum Using Conjugated Polyelectrolytes. *J. Mater. Chem.* **2007**, *17*, 3702−3707.
(11) Pearce, D. A.; Walkup, G. K.; Imperiali, B. Peptidyl Chemosensors Incorporating A Fret Mechanism for Detection of Ni(II). *Bioorg. Med. Chem. Lett.* **1998**, *8*, 1963−1968.
(12) Jiang, G.; Susha, A. S.; Lutich, A. A.; Stefani, F. D.; Feldmann, J.; Rogach, A. L. Cascaded FRET in Conjugated Polymer/Quantum Dot/Dye-Labeled DNA Complexes for DNA Hybridization Detection. *ACS Nano* **2009**, *3*, 4127−4131.
(13) Wang, F.; Banerjee, D.; Liu, Y.; Chen, X.; Liu, X. Upconversion Nanoparticles in Biological Labeling, Imaging, and Therapy. *Analyst* **2010**, *135*, 1839−1854.
(14) Feng, X.; Liu, L.; Wang, S.; Zhu, D. Water-Soluble Fluorescent Conjugated Polymers and Their Interactions with Biomacromolecules for Sensitive Biosensors. *Chem. Soc. Rev.* **2010**, *39*, 2411−2419.
(15) Zhu, C.; Liu, L.; Yang, Q.; Lv, F.; Wang, S. Water-Soluble Conjugated Polymers for Imaging, Diagnosis, and Therapy. *Chem. Rev.* **2012**, *112*, 4687−4735.
(16) Park, S. Y.; Kim, S. H.; Lee, M. H.; No, K.; Lee, J. H.; Kim, J. S. Fe(III)-Induced FRET-On: Energy Transfer from Rhodamine 6G to Nile Red. *Bull. Korean Chem. Soc.* **2011**, *32*, 741−744.
(17) Chen, G.; Song, F.; Xiong, X.; Peng, X. Fluorescent Nanosensors Based on Fluorescence Resonance Energy Transfer (FRET). *Ind. Eng. Chem. Res.* **2013**, *52*, 11228−11245.
(18) Sanches, J. M.; Rodrigues, I. A Photobleaching/Photoblinking Analytical Model for LSFCM Imaging. *Microsc. Microanal.* **2013**, *19*, 81−82.
(19) Tuncel, D.; Demir, H. V. Conjugated Polymer Nanoparticles. *Nanoscale* **2010**, *2*, 484−494.
(20) An, B.-K.; Kwon, S.-K.; Jung, S.-D.; Park, S. Y. Enhanced Emission and Its Switching in Fluorescent Organic Nanoparticles. *J. Am. Chem. Soc.* **2002**, *124*, 14410−14415.
(21) Horn, D.; Rieger, J. Organic Nanoparticles in the Aqueous Phase-Theory, Experiment, and Use. *Angew. Chem., Int. Ed.* **2001**, *40*, 4330−4361.
(22) Fisslthaler, E.; Sax, S.; Scherf, U.; Mauthner, G.; Moderegger, E.; Landfester, K.; List, E. J. Inkjet Printed Polymer Light-Emitting Devices Fabricated by Thermal Embedding of Semiconducting Polymer Nanospheres in An Inert Matrix. *Appl. Phys. Lett.* **2008**, *92*, 183305.
(23) Wu, C.; Szymanski, C.; McNeill, J. Preparation and Encapsulation of Highly Fluorescent Conjugated Polymer Nanoparticles. *Langmuir* **2006**, *22*, 2956−2960.
(24) Chen, J.; Law, C. C.; Lam, J. W.; Dong, Y.; Lo, S. M.; Williams, I. D.; Zhu, D.; Tang, B. Z. Synthesis, Light Emission, Nanoaggregation, and Restricted Intramolecular Rotation of 1, 1-Substituted 2, 3, 4, 5-Tetraphenylsiloles. *Chem. Mater.* **2003**, *15*, 1535−1546.
(25) Han, M.; Hara, M. Intense Fluorescence from Light-Driven Self-Assembled Aggregates of Nonionic Azobenzene Derivative. *J. Am. Chem. Soc.* **2005**, *127*, 10951−10955.
(26) Yasukuni, R.; Asahi, T.; Sugiyama, T.; Masuhara, H.; Sliwa, M.; Hofkens, J.; De Schryver, F.; Van der Auweraer, M.; Herrmann, A.; Müllen, K. Fabrication of Fluorescent Nanoparticles of Dendronized Perylenediimide by Laser Ablation in Water. *Appl. Phys. A: Mater. Sci. Process.* **2008**, *93*, 5−9.
(27) Xu, X.; Chen, S.; Li, L.; Yu, G.; Di, C.; Liu, Y. Photophysical Properties of Polyphenylphenyl Compounds in Aqueous Solutions and Application of Their Nanoparticles for Nucleobase Sensing. *J. Mater. Chem.* **2008**, *18*, 2555−2562.
(28) Zheng, C.; Xu, X.; He, F.; Li, L.; Wu, B.; Yu, G.; Liu, Y. Preparation of High-Quality Organic Semiconductor Nanoparticle Films by Solvent-Evaporation-Induced Self-Assembly. *Langmuir* **2010**, *26*, 16730−16736.
(29) Wang, J.; Xu, X.; Shi, L.; Li, L. Fluorescent Organic Nanoparticles Based on Branched Small Molecule: Preparation and Ion Detection in Lithium-Ion Battery. *ACS Appl. Mater. Interfaces* **2013**, *5*, 3392−3400.
(30) Tang, F.; Wang, C.; Wang, J.; Wang, X.; Li, L. Fluorescent Organic Nanoparticles with Enhanced Fluorescence by Self-aggregation and Their Application to Cellular Imaging. *ACS Appl. Mater. Interfaces* **2014**, *6*, 18337−18343.
(31) Li, K.; Liu, B. Polymer-Encapsulated Organic Nanoparticles for Fluorescence and Photoacoustic Imaging. *Chem. Soc. Rev.* **2014**, *43*, 6570−6597.
(32) Li, L.; Shen, X.; Xu, Q.-H.; Yao, S. Q. A Switchable Two-Photon Membrane Tracer Capable of Imaging Membrane-Associated Protein Tyrosine Phosphatase Activities. *Angew. Chem., Int. Ed.* **2013**, *52*, 424−428.
(33) Wang, X.; He, F.; Li, L.; Wang, H.; Yan, R.; Li, L. Conjugated Oligomer-Based Fluorescent Nanoparticles as Functional Nanocarriers for Nucleic Acids Delivery. *ACS Appl. Mater. Interfaces* **2013**, *5*, 5700−5708.
(34) Feng, X.; Tang, Y.; Duan, X.; Liu, L.; Wang, S. Lipid-Modified Conjugated Polymer Nanoparticles for Cell Imaging and Transfection. *J. Mater. Chem.* **2010**, *20*, 1312−1316.
(35) Yuan, H.; Liu, Z.; Liu, L.; Lv, F.; Wang, Y.; Wang, S. Cationic Conjugated Polymers for Discrimination of Microbial Pathogens. *Adv. Mater.* **2014**, *26*, 4333−4338.
(36) Wang, L.; Dong, L.; Bian, G.-R.; Wang, L.-Y.; Xia, T.-T.; Chen, H.-Q. Using Organic Nanoparticle Fluorescence to Determine Nitrite in Water. *Anal. Bioanal. Chem.* **2005**, *382*, 1300−1303.
(37) Grimland, J. L.; Wu, C.; Ramoutar, R. R.; Brumaghim, J. L.; McNeill, J. Photosensitizer-Doped Conjugated Polymer Nanoparticles with High Cross-Sections for One-and Two-Photon Excitation. *Nanoscale* **2011**, *3*, 1451−1455.
(38) Kim, H. Y.; Bjorklund, T.; Lim, S.-H.; Bardeen, C. Spectroscopic and Photocatalytic Properties of Organic Tetracene Nanoparticles in Aqueous Solution. *Langmuir* **2003**, *19*, 3941−3946.
(39) Zhou, Y.; Bian, G.; Wang, L.; Dong, L.; Wang, L.; Kan, J. Sensitive Determination of Nucleic Acids Using Organic Nanoparticle Fluorescence Probes. *Spectrochim. Acta, Part A* **2005**, *61*, 1841−1845.
(40) De, M.; Ghosh, P. S.; Rotello, V. M. Applications of Nanoparticles in Biology. *Adv. Mater.* **2008**, *20*, 4225−4241.
(41) Howes, P.; Green, M.; Levitt, J.; Suhling, K.; Hughes, M. Phospholipid Encapsulated Semiconducting Polymer Nanoparticles: Their Use in Cell Imaging and Protein Attachment. *J. Am. Chem. Soc.* **2010**, *132*, 3989−3996.
(42) Feng, X.; Yang, G.; Liu, L.; Lv, F.; Yang, Q.; Wang, S.; Zhu, D. A Convenient Preparation of Multi-Spectral Microparticles by Bacteria-Mediated Assemblies of Conjugated Polymer Nanoparticles for Cell Imaging and Barcoding. *Adv. Mater.* **2012**, *24*, 637−641.
(43) Ray, P. C.; Darbha, G. K.; Ray, A.; Walker, J.; Hardy, W. Gold Nanoparticle Based FRET for DNA Detection. *Plasmonics* **2007**, *2*, 173−183.
(44) Chatterjee, D. K.; Gnanasammandhan, M. K.; Zhang, Y. Small Upconverting Fluorescent Nanoparticles for Biomedical Applications. *Small* **2010**, *6*, 2781−2795.
(45) Liu, B.; Bazan, G. C. Homogeneous Fluorescence-Based DNA Detection with Water-Soluble Conjugated Polymers. *Chem. Mater.* **2004**, *16*, 4467−4476.

DOI: 10.1021/acsami.5b01338
ACS Appl. Mater. Interfaces 2015, 7, 8243−8250

(46) Zhao, X.; Tapec-Dytioco, R.; Tan, W. Ultrasensitive DNA Detection Using Highly Fluorescent Bioconjugated Nanoparticles. *J. Am. Chem. Soc.* **2003**, *125*, 11474−11475.
(47) Clegg, R. M. Fluorescence Resonance Energy Transfer. *Curr. Opin. Biotechnol.* **1995**, *6*, 103−110.
(48) Whitehead, K. S.; Grell, M.; Bradley, D. D. C.; Jandke, M.; Strohriegl, P. Highly Polarized Blue Electroluminescence from Homogeneously Aligned Films of Poly(9,9-dioctylfluorene). *Appl. Phys. Lett.* **2000**, *76*, 2946−2948.
(49) Bao, B.; Tao, N.; Yang, D.; Yuwen, L.; Weng, L.; Fan, Q.; Huang, W.; Wang, L. A Controllable Approach to Development of Multi-Spectral Conjugated Polymer Nanoparticles with Increased Emission for Cell Imaging. *Chem. Commun.* **2013**, *49*, 10623−10625.
(50) Zhang, X.; Wang, Y.; Ma, Y.; Ye, Y.; Wang, Y.; Wu, K. Solvent-Stabilized Oxovanadium Phthalocyanine Nanoparticles and Their Application in Xerographic Photoreceptors. *Langmuir* **2006**, *22*, 344−348.
(51) Schnurmann, R. Contact Electrification of Solid Particles. *Proc. Phys. Soc., London* **1941**, *53*, 547.
(52) Moynihan, S.; Lovera, P.; O'Carroll, D.; Iacopino, D.; Redmond, G. Alignment and Dynamic Manipulation of Conjugated Polymer Nanowires in Nematic Liquid Crystal Hosts. *Adv. Mater.* **2008**, *20*, 2497−2502.
(53) Förster, T. Energiewanderung und Fluoreszenz. *Naturwissenschaften* **1946**, *33*, 166−175.
(54) Langmuir, I. The Adsorption of Gases on Plane Surfaces of Glass, Mica and Platinum. *J. Am. Chem. Soc.* **1918**, *40*, 1361−1403.
(55) Bird, P. G. A Derivation of Langmuir's Adsorption Isotherm. *J. Chem. Educ.* **1933**, *10*, 237.

DOI: 10.1021/acsami.5b01338
ACS Appl. Mater. Interfaces 2015, 7, 8243−8250